Title
PAR1 contributes to influenza A virus pathogenicity in mice

Journal
Journal of Clinical Investigation, 123(1)

ISSN
0021-9738

Authors
Khoufache, Khaled
Berri, Fatma
Nacken, Wolfgang
et al.

Publication Date
2013-01-02

DOI
10.1172/jci61667

Peer reviewed

PAR1 contributes to influenza A virus pathogenicity in mice

Khaled Khoufache,[1,2] Fatma Berri,[1] Wolfgang Nacken,[3] Annette B. Vogel,[4,5] Marie Delenne,[1] Eric Camerer,[6,7] Shaun R. Coughlin,[8] Peter Carmeliet,[9,10] Bruno Lina,[1] Guus F. Rimmelzwaan,[11] Oliver Planz,[4] Stephan Ludwig,[3] and Béatrice Riteau[1,2]

[1]Virologie et Pathologie Humaine, EA 4610, Université Lyon1, Faculté de Médecine RTH Laennec, Lyon, France. [2]INRA Tours, Nouzilly, France. [3]Institute of Molecular Virology, ZMBE, Westfälische-Wilhelms-University, Münster, Germany. [4]Friedrich-Loeffler-Institute, Institute of Immunology, University Hospital, Tuebingen, Germany. [5]Institute of Immunology, Friedrich-Loeffler-Institut, Greifswald-Insel Riems, Germany. [6]INSERM U970, Paris Cardiovascular Centre, Paris, France. [7]Université Paris-Descartes, Paris, France. [8]Cardiovascular Research Institute, UCSF, San Francisco, California, USA. [9]Laboratory of Angiogenesis and Neurovascular link, Vesalius Research Center, VIB, Leuven, Belgium. [10]Laboratory of Angiogenesis and Neurovascular link, Vesalius Research Center, KU Leuven, Leuven, Belgium. [11]Department of Virology, Erasmus Medical Center, Rotterdam, the Netherlands.

Influenza causes substantial morbidity and mortality, and highly pathogenic and drug-resistant strains are likely to emerge in the future. Protease-activated receptor 1 (PAR1) is a thrombin-activated receptor that contributes to inflammatory responses at mucosal surfaces. The role of PAR1 in pathogenesis of virus infections is unknown. Here, we demonstrate that PAR1 contributed to the deleterious inflammatory response after influenza virus infection in mice. Activating PAR1 by administering the agonist TFLLR-NH_2 decreased survival and increased lung inflammation after influenza infection. Importantly, both administration of a PAR1 antagonist and PAR1 deficiency protected mice from infection with influenza A viruses (IAVs). Treatment with the PAR1 agonist did not alter survival of mice deficient in plasminogen (PLG), which suggests that PLG permits and/or interacts with a PAR1 function in this model. PAR1 antagonists are in human trials for other indications. Our findings suggest that PAR1 antagonism might be explored as a treatment for influenza, including that caused by highly pathogenic H5N1 and oseltamivir-resistant H1N1 viruses.

Introduction

Influenza is an ineradicable contagious disease that occurs in seasonal epidemics and sporadic pandemic outbreaks that pose significant morbidity and mortality for humans and animals (1–3). The continuous sporadic infections of humans with highly pathogenic avian influenza viruses of the H5N1 subtype and the recent pandemic caused by swine-origin H1N1 viruses highlight the permanent threat caused by these viruses (4–6). The pathogenesis of influenza A virus (IAV) infection is not fully understood, but involves both viral traits and the host immune response (3). Full understanding of the host response may aid in the development of intervention strategies that target these host factors.

Both innate and adaptive components of the immune system are activated shortly after virus infection, which provides an efficient line of defense against IAV (7). However, excessive inflammation may also result in lung damage that limits respiratory capacity and may account for IAV pathogenesis in humans (1, 8, 9). Recruitment of inflammatory cells to inflamed sites is controlled by a number of cellular components, including proteases (10). These proteases not only cleave extracellular substrates, but also mediate signal transduction in part via protease-activated receptors (PARs) (11–14). PAR1, which links local protease activity to cellular responses involved in thrombosis, inflammation, and cytoprotection (15, 16), shows increased expression in the airways of IAV-infected mice (17). The role of PAR1 in the context of IAV infection has not been studied. We report evidence that PAR1 signaling contributed to the deleterious inflammation that followed influenza virus infection in mice in a manner dependent on plasminogen (PLG). While administration of a PAR1 agonist to mice increased severity of IAV infection, PAR1 deficiency protected mice from fatal outcome. Administration of the PAR1 antagonist SCH79797 (18) to mice decreased inflammation and improved survival after infection with multiple IAV strains, including a highly pathogenic avian H5N1 strain and 2009 pandemic H1N1 virus. Importantly, administration of SCH79797 improved survival in mice even when administered 48 or 72 hours after inoculation. PAR1 antagonists are currently in clinical trials for potential use as antithrombotic drugs (19–22). Because an intervention strategy aimed at a host cellular protein would be effective against virus strains that develop resistance to existing antiviral drugs, PAR1 antagonists might be explored for the treatment of IAV in additional preclinical models and, if appropriate, in humans.

Results

PAR1 contributes to the pathogenesis of IAV infection. To investigate the role of PAR1 in the pathogenesis of IAV infection, WT mice were inoculated with 50 or 500 PFU of H1N1 strain A/PR/8/34 (referred to herein as H1N1) and either left untreated or stimulated with 50 μM of the PAR1 agonist TFLLR-NH_2 (referred to herein as PAR1-activating peptide; PAR1-AP). Mice treated with PAR1-AP displayed enhanced weight loss and higher mortality rates after infection compared with untreated control mice, differences that were statistically significant at both doses (Figure 1A). In contrast, treatment of uninfected mice with PAR1-AP did not affect survival or body weight of mice (Figure 1B), which indicates that the effect of PAR1-AP on survival and weight loss requires IAV infection.

Authorship note: Khaled Khoufache and Fatma Berri contributed equally to this work.

Conflict of interest: Khaled Khoufache and Béatrice Riteau have a patent concerning the use of PAR1 antagonist against influenza.

Citation for this article: *J Clin Invest.* 2013;123(1):206–214. doi:10.1172/JCI61667.

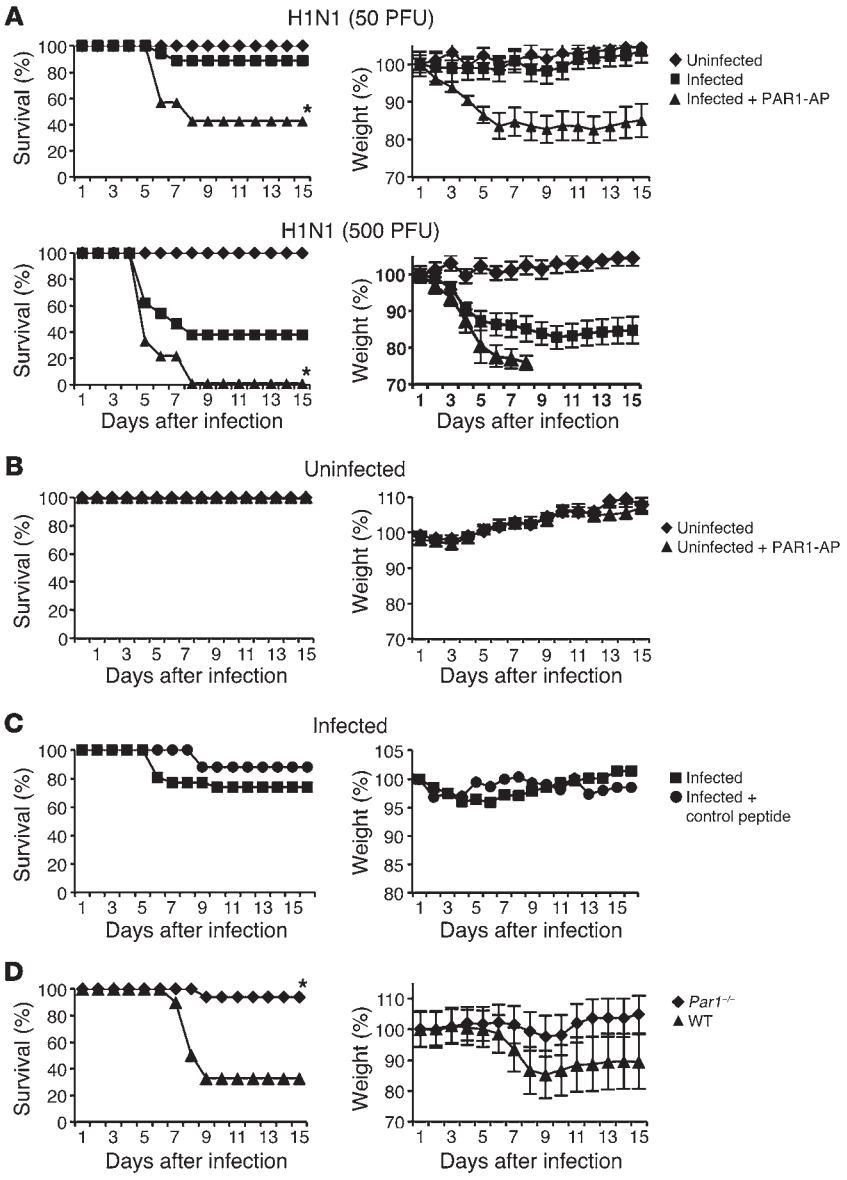

Figure 1
Effect of PAR1 activation and PAR1 deficiency on IAV pathogenicity. (**A**) Time course of IAV-induced pathogenesis and death in mice in response to PAR1 stimulation. Mice were inoculated intranasally with H1N1 (50 PFU, n = 22 per group; 500 PFU, n = 18 per group) and treated with either vehicle or 50 μM PAR1-AP. (**B**) Time course of uninfected mice treated or not with 50 μM PAR1-AP (n = 13 per group). (**C**) Mice were infected with 50 PFU H1N1 and treated with control peptide or vehicle (n = 10 per group). Results are average percent survival or weight loss from 3 independent experiments. (**D**) Survival and weight loss of *Par1*$^{-/-}$ mice and WT littermates after infection with 100 PFU H1N1 (n = 12 per group). Results are average percent survival or weight loss from 2 experiments. $P < 0.05$, PAR1-AP vs. untreated or *Par1*$^{-/-}$ vs. WT, Kaplan-Meier test.

Moreover, treatment with a control peptide did not impair survival or increase weight loss in IAV-infected mice (Figure 1C), militating against nonspecific effects of peptide administration. Thus, PAR1 activation led to increased pathogenicity of IAV infection.

To further explore the role of PAR1 in IAV pathogenesis, we investigated the consequence of PAR1 deficiency. *Par1*$^{+/-}$ mice were intercrossed to generate WT and *Par1*$^{-/-}$ mice, which were infected with 100 PFU H1N1, and weight loss and survival rates were monitored. Compared with WT littermates, *Par1*$^{-/-}$ mice were more resistant to IAV infection (Figure 1D). Thus, PAR1 contributed to death and weight loss caused by IAV infection.

PAR1-AP increases cytokine release and neutrophil recruitment in the lungs of infected mice. Because PAR1 can trigger cytokine production in endothelial and other cell types (14), we next investigated the effects of PAR1-AP in the inflammatory response induced by IAV infection. Mice infected with 50 PFU H1N1 were treated or not with 50 μM PAR1-AP, and bronchoalveolar lavages (BALs) were collected to assess the presence of cytokines and polymorphonuclear neutrophils (PMNs) in the lungs at different time points after inoculation. IAV infection resulted in increased levels of all cytokines tested (RANTES, IL-6, and KC) in a time course–dependent manner, and PAR1-AP treatment augmented this response (Figure 2A). Similar results were obtained when the effect of PAR1 was compared with that of a control peptide (Supplemental Figure 1; supplemental material available online with this article; doi:10.1172/JCI61667DS1), confirming PAR1-AP specificity. PAR1-AP treatment also increased the occurrence of BAL PMNs 24 and 48 hours after infection, but had little effect in uninfected mice (Figure 2B). By 72 hours after infection, the PMN content of BAL in PAR1-AP–treated and control mice was not different. These results suggest that PAR1 activation can increase IAV-induced production of cytokines and increase early recruitment of neutrophils in the lungs of infected mice.

Virus replication in the lungs. We then investigated whether the effect of PAR1 activation on the outcome of IAV infection in mice correlates with an increase of virus production in the lungs. To this end,

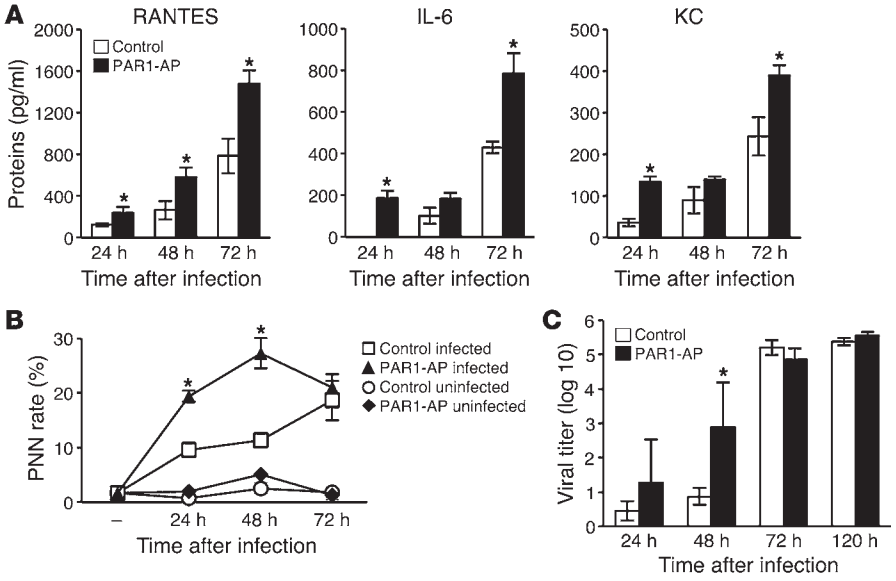

Figure 2
PAR1-AP increases inflammation and virus replication during 50 PFU H1N1 infection in mice. (**A**) Cytokines in the BAL of infected mice treated or not with PAR1-AP were measured by ELISA 24, 48, and 72 hours after inoculation. Data are mean ± SD from 5–11 individual animals per group from 3 experiments. (**B**) Relative PMN numbers in BAL from infected mice treated or not with PAR1-AP. PMN percentage was determined by May-Grünwald–Giemsa staining 24, 48, or 72 hours after inoculation. Results are mean ± SD from 4–5 individual mice per group from 2 individual experiments. Noninfected mice were used as control (n = 2–4 per group). (**C**) H1N1 virus titers in the lungs at the indicated times after infection of mice treated or not with 50 μM PAR1-AP. Data are average ± SD from 3–5 individual animals per group. *P < 0.05, treated vs. untreated, Mann-Whitney test.

infectious virus titers were determined in lungs collected from mice treated with PAR1-AP (50 μM) or control peptide at different time points after inoculation. At 24 and 48 hours after inoculation, virtually no virus replication was detected (10^1 was the detection limit of the assay), but lung virus titers significantly increased after PAR1-AP treatment (Figure 2C). No significant differences were observed 3 and 5 days after infection. These data suggest that PAR1 activation promotes an early increase in virus production in mouse lungs.

The effect of PAR1 activation on virus production, weight loss, and survival after IAV infection is PLG dependent. To decipher the mechanism by which PAR1 accelerated virus production in vivo, we performed in vitro experiments to assess the effect of PAR1 activation on virus replication in alveolar epithelial A549 cells. PAR1-AP triggered ERK phosphorylation in these cells, with a maximal effect at about 40 μM (Figure 3A); this concentration was used in all subsequent in vitro experiments. Because proteolytic cleavage of HA is essential for IAV infectivity, and PLG promotes IAV replication through HA cleavage (23, 24), we examined the effect of adding PLG — alone or in combination with PAR1-AP — on virus production. As expected, viral production was barely detectable in untreated A549 cultures, but was markedly increased by the addition of PLG (Figure 3B). Importantly, addition of PAR1-AP augmented this effect 8 and 24 hours after infection. The effect of PAR1-AP was not seen when trypsin was used as an alternative protease for IAV replication (data not shown), and PAR1 signaling did not affect virus entry into cells (Supplemental Figure 2). However, inclusion of PAR1-AP appeared to increase PLG-dependent cleavage of HA. Thus, we next infected A549 cells (MOI 0.5) in the presence or absence of PLG, with or without PAR1-AP, and evaluated HA cleavage by Western blot analysis 16 hours after infection. In the absence of PLG, similar amounts of uncleaved HA (HA_0) accumulated in infected cells, and PAR1-AP was without effect (Figure 3C). In the presence of PLG, in addition to HA_0, a 25-kDa band corresponding to HA_2 was observed. Importantly, in PAR1-AP–treated cultures, the intensity of HA_2 increased and HA_0 decreased relative to that in control cultures. Thus, viral HA was cleaved in a PLG-dependent manner that was enhanced by PAR1-AP and correlated with increased viral production.

PLG is an important mediator of lung inflammation (25, 26) and is known to influence IAV virulence (27, 28). Importantly, PLG binding to cells and activation may be controlled by PAR1 signaling (29, 30). In combination with the findings outlined above, these observations prompted us to investigate whether the effect of PAR1 signaling on the pathogenicity of IAV infection also depends on PLG in vivo. We therefore inoculated $Plg^{-/-}$ mice with 50 PFU H1N1 with or without PAR1-AP treatment. In contrast to WT mice, treatment of $Plg^{-/-}$ mice with PAR1-AP did not increase mortality rates, weight loss, or virus titers in lungs after IAV infection (Figure 3, D and E).

Histopathological examination showed that treatment with PAR1-AP increased cellular infiltrates in lungs from infected WT mice, but not $Plg^{-/-}$ mice (Supplemental Figure 3). These results suggest that PAR1 activation increased early virus production, inflammation, and pathogenicity of IAV infection in a PLG-dependent fashion. Notably, when this low 50-PFU dose was used, virtually no virus replication was detected in the lungs of WT or $Plg^{-/-}$ mice at the indicated time points after inoculation (Figure 3E). Additionally, leukocyte infiltration in IAV-infected WT or $Plg^{-/-}$ mice was barely detectable (Supplemental Figure 3). However, when a higher virus dose was used for inoculation, leukocyte infiltration and lung virus titers of $Plg^{-/-}$ mice were substantially lower than those of WT mice (F. Berri, unpublished observations), which suggests that PLG promotes IAV replication and inflammation. While the finding that PAR1-AP increased PLG-dependent cleavage of HA in vitro suggests that PAR1 signaling might promote viral replication by enhancing PLG/plasmin function, our data do not exclude a PAR1-independent permissive role for PLG or PLG-independent roles for PAR1 activation in IAV infection and pathogenesis.

PAR1 antagonist protects against H1N1 and H3N2 infection. We next investigated whether pharmacological inhibition of PAR1 signaling alters the course of IAV infection. The pharmacology of PARs is not well developed, and inhibitors capable of blocking PAR1 function in mouse models have not been well characterized with respect to off-target effects. Nonetheless, SCH79797 has been used to probe PAR1 function in rodent models (31–33); thus, encouraged by the protection against IAV seen in $Par1^{-/-}$ mice, we examined the effects of this compound on the course of IAV infection.

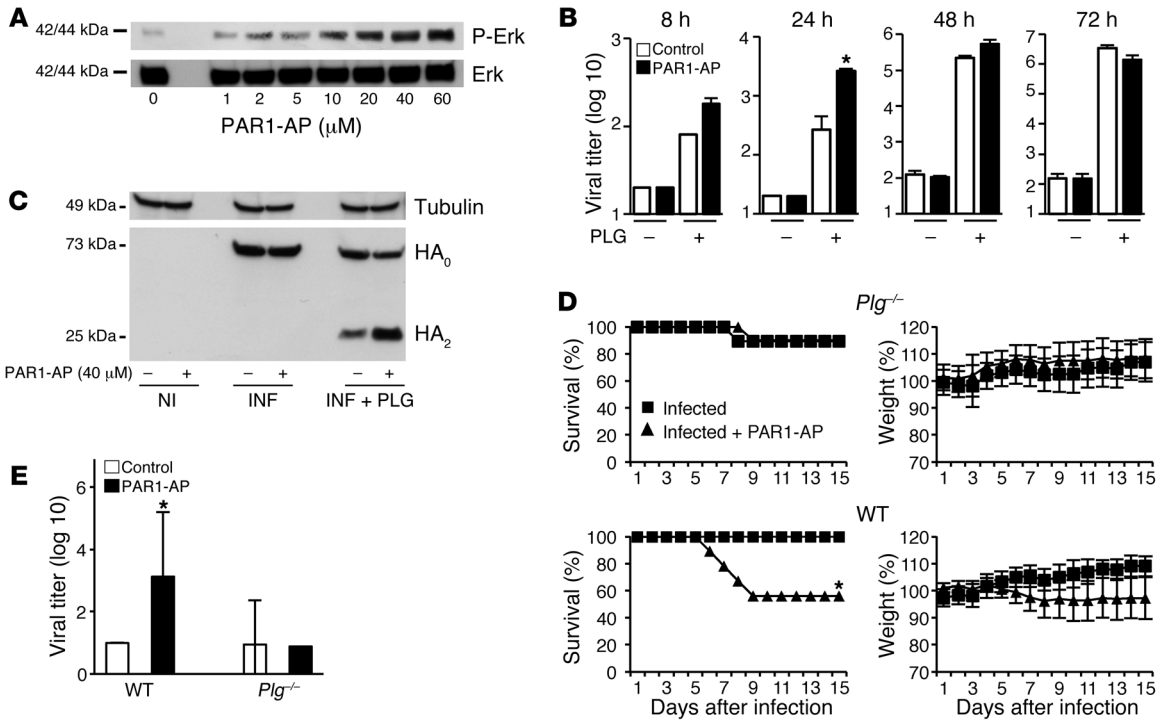

Figure 3

Effect of PLG and PLG deficiency on IAV production and PAR1-AP effects. (**A**) ERK phosphorylation after stimulation of A549 cells with the indicated PAR1-AP concentrations. Anti–phospho-Erk and anti-Erk antibodies were used. (**B**) Infectious virus titers in the supernatant of infected cells after stimulation with 40 μM PAR1-AP or control peptide in the presence or absence of PLG. (**C**) Noninfected (NI) or infected (INF) cells were stimulated with 40 μM PAR1-AP or control peptide in the presence or absence of PLG. After cell lysis, proteins were analyzed by Western blot for HA cleavage. (**D**) Time course of IAV-induced pathogenesis in *Plg*$^{-/-}$ and WT littermates after treatment or not with PAR1-AP (n = 9–10 mice per group from 2 experiments). (**E**) Virus titers 48 hours after infection (50 PFU) in lungs of WT or *Plg*$^{-/-}$ mice stimulated or not with 50 μM PAR1-AP. Data are average ± SD from 5 individual animals per group from 2 experiments. *P < 0.05, treated vs. untreated, Kaplan-Meier test (**D**), Mann Whitney test (**B** and **E**).

SCH79797 inhibited PAR1-AP–induced ERK activation in mouse NIH3T3 cells (Figure 4A), which suggests that it is capable of blocking signaling by the mouse homolog of PAR1. SCH79797 treatment prevented decreased survival and increased weight loss associated with administration of PAR1-AP to IAV-infected mice (Figure 4B). More strikingly, when mice were infected with lethal doses of H1N1 (500 and 5,000 PFU), SCH79797 treatment protected mice from weight loss and death: 47% and 16% survival, respectively, was observed in untreated control mice, whereas 84%–94% of SCH79797-treated mice survived the infections (Figure 4C). Moreover, when SCH79797 was administered beginning 2 or 3 days after infection, mice were also significantly protected from H1N1 and from H3N2 strain A/Hong-Kong/68 (referred to herein as H3N2; Figure 4, D and E). Treatment of uninfected mice with SCH79797 did not affect their survival rates or body weight (Supplemental Figure 4), which suggests that PAR1 antagonists do not cause side effects. Thus, SCH79797 treatment protected mice from IAV infection, consistent with the notion that PAR1 contributes to IAV pathogenesis in this model.

Inflammation and virus replication are attenuated by SCH79797. Since PAR1 activation promoted inflammation in the lungs during IAV infection, we determined whether blockade of PAR1 signaling would result in reduced IAV-induced inflammation in vivo. Mice were infected with 500 PFU H1N1 and treated or not with SCH79797, and BAL was collected at different times after inoculation. SCH79797 treatment significantly reduced the levels of RANTES, IL-6, and KC in BAL 24, 48, and 72 hours after inoculation, as measured by ELISA (Figure 5A). 5 days after inoculation, cytokine levels were still high in the BAL from untreated mice, but barely detectable in the BAL from SCH79797-treated mice (Supplemental Figure 5). SCH79797 treatment also significantly decreased PMN frequency in the BAL of infected mice: 24 and 48 hours after inoculation, PMNs were hardly detectable in the BAL of SCH79797-treated mice, whereas they represented 10% of cells in BAL from untreated mice (Figure 5B). Accordingly, histopathological examination revealed a reduction of cell infiltration in the lungs of infected mice treated with SCH79797 (Supplemental Figure 6).

Finally, a reduction in lung virus titers was observed 24 and 48 hours after 500 PFU H1N1 inoculation compared with untreated controls (Figure 5C). At day 3 after inoculation, lung virus titers were similar in SCH79797-treated and untreated mice (approximately 10^4 PFU/ml), which suggests that SCH79797 delayed, but did not prevent, virus production. Lung virus titers dropped to less than 10^2 PFU/ml at days 5 and 7 in both SCH79797-treated and control mice (Figure 5C). The observation that SCH79797 suppressed markers of inflammation, but not viral titers, at day 3 suggests that inhibition of PAR1 signaling may inhibit inflammation and early virus replication by at least partially independent mechanisms.

SCH79797 protects against highly pathogenic H1N1v and H5N1 infection. To test whether inhibition of PAR1 signaling by SCH79797

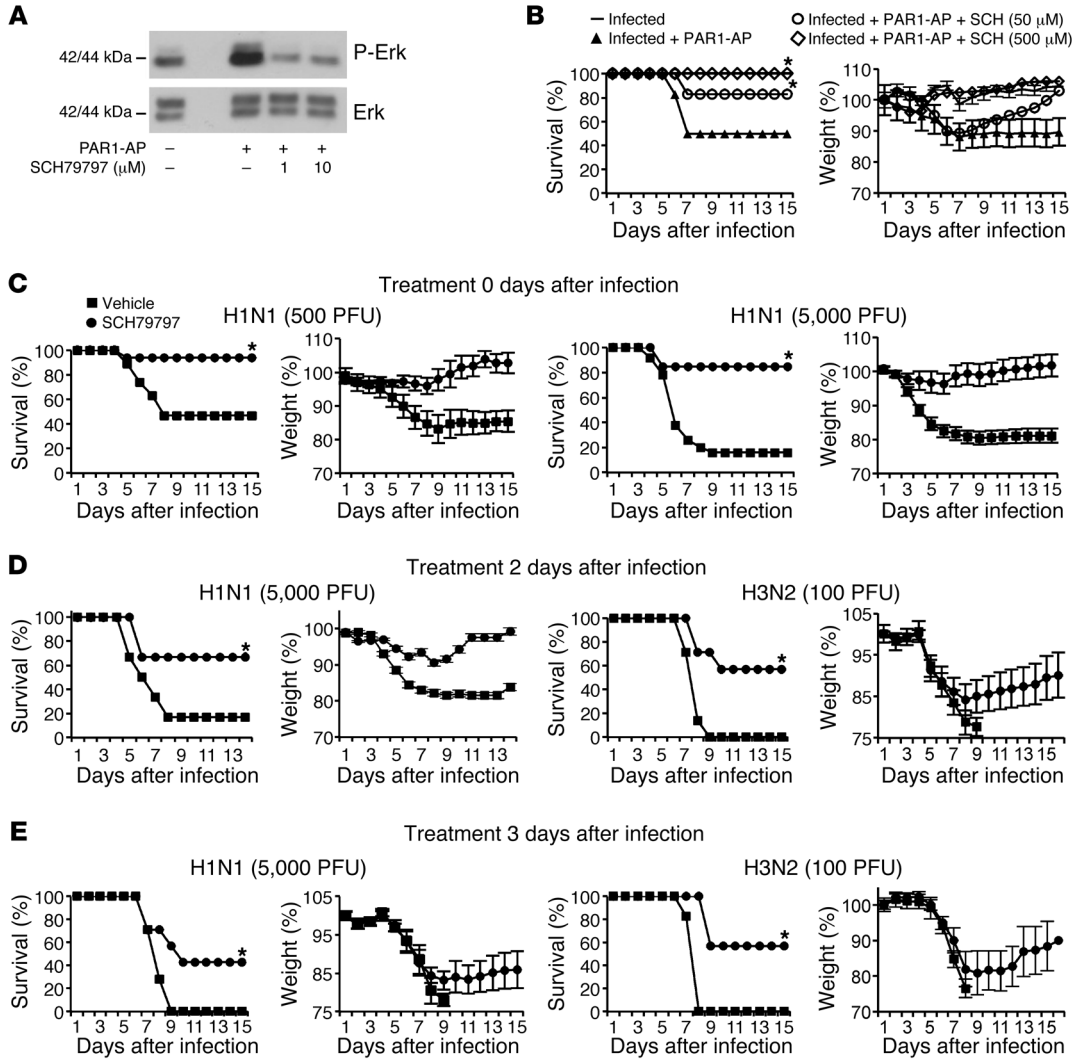

Figure 4

PAR1 antagonist protects mice against infection with H1N1 and H3N2. (**A**) Treatment of NIH3T3 cells with SCH79797 blocked ERK activation by 10 μM PAR1-AP. (**B**) SCH79797 treatment prevented PAR1-AP–induced mouse mortality in a dose-dependent manner. (**C**) IAV-induced pathogenesis in infected mice treated or not with SCH79797. Mice were inoculated with 500 PFU (n = 17–19 per group) or 5,000 PFU (n = 14 per group) H1N1 and treated or not with 50 μM SCH79797 on days 0–2 after infection. (**D**) SCH79797 treatment on days 2–4 after infection with 5,000 PFU H1N1 (n = 12 per group) or 100 PFU H3N2 (n = 7 per group). (**E**) SCH79797 treatment on days 3–5 after infection with 5,000 PFU H1N1 (n = 7 per group) or 100 PFU H3N2 (n = 7 per group). *P < 0.05, treated vs. control, Kaplan-Meier test.

also affects infection with other IAV strains, mice were infected with a highly pathogenic H5N1 strain or a pandemic H1N1v strain that had acquired oseltamivir resistance during treatment of a severe infection (see Methods and ref. 34), then treated or not with SCH79797. After lethal infection with 5,000 PFU H5N1 and 500 PFU H1N1v, 60% and 100% of untreated control mice died, respectively, whereas almost full protection was observed in SCH79797-treated animals of both inoculation groups (P < 0.05; Figure 6, A and B). In addition to mortality and body weight, the onset of clinical signs was also inhibited when H5N1-infected mice were treated with SCH79797 compared with untreated mice (data not shown). Mouse mortality was monitored until day 21 after inoculation, and sustained survival was observed after SCH79797 treatment (data not shown), which indicated that SCH79797 protection was durable. Thus, inhibition of PAR1 signaling protected mice against infection with various IAVs, including highly pathogenic strains.

Discussion

Our present findings support an important role for PAR1 in mouse models of IAV infection. Studies with PAR1-AP indicated that PAR1 activation increased inflammation, early virus production, weight loss, and mortality after infection (Figures 1 and 2), and studies using *Par1*$^{-/-}$ mice indicated that PAR1 contributed to the pathogenesis of IAV infection (Figure 1). The observation that SCH79797, a drug that inhibits PAR1 signaling, decreased inflammation, early virus production, weight loss, and mortality after infection was in accord with the PAR1-AP and *Par1*$^{-/-}$ results. Moreover, the observation that SCH79797 decreased mortality after infection with multiple IAV strains (H1N1, H3N2, and

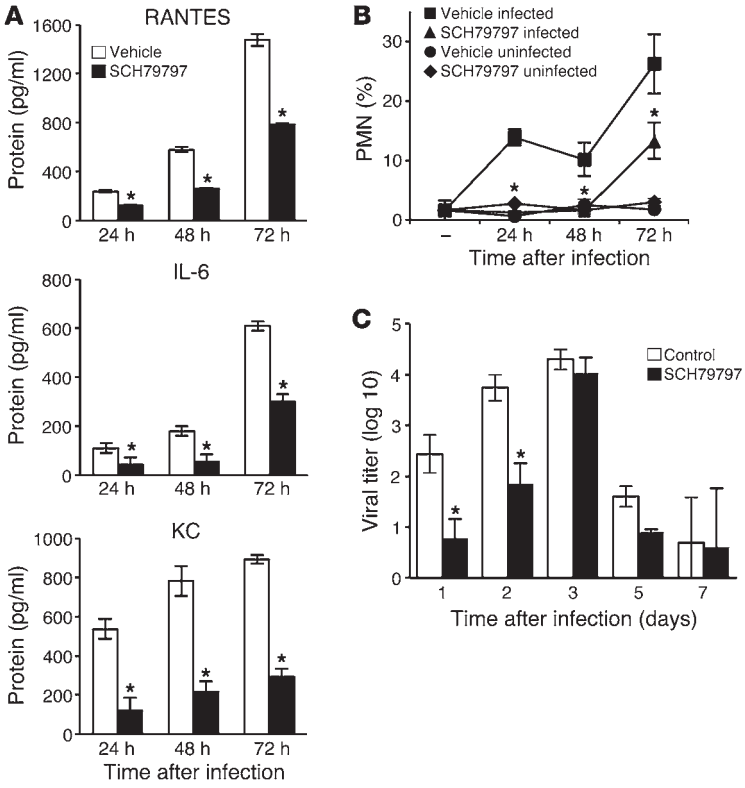

Figure 5
PAR1 antagonist inhibits lung inflammation and virus replication. (**A**) Cytokines in the BAL of infected mice treated or not with SCH79797 were measured by ELISA 24, 48, and 72 hours after inoculation. Data are average ± SD from 7–11 individual animals per group, representative of 3 experiments. (**B**) Relative PMN frequency in BAL from infected mice treated or not with SCH79797. PMN percentage was determined by May-Grünwald–Giemsa staining 24, 48, and 72 hours after inoculation. Data are average ± SD from 3–5 individual mice per group. Noninfected mice were used as control (n = 3–5 per group). Results are representative of 2 individual experiments. (**C**) Virus titers in lungs of infected mice at the indicated times after infection with 500 PFU H1N1 and treatment with SCH79797. Data are average ± SD from 3–5 individual animals per group. *P < 0.05, treated vs. control, Mann-Whitney test.

H5N1), and was effective even when dosing was initiated at day 3 after inoculation, suggests that PAR1 inhibition should be explored in additional preclinical studies and, if appropriate, in humans as a possible treatment for influenza.

To our knowledge, a role for PAR1 in the response to, and the pathogenesis of, virus infections has not been previously described. PAR1 activation in endothelial cells, fibroblasts, and other cell types triggers various responses, many of which are proinflammatory (e.g., chemokine and cytokine production, adhesion molecule display, prostaglandin production, and permeability increases; refs. 14, 15). In accord with our observations, intratracheal delivery of PAR1 agonist was not sufficient to trigger inflammation in the lungs of otherwise normal mice (35), but did exacerbate ventilation injury–induced pulmonary edema (36). Additionally, *Par1*$^{-/-}$ mice are protected from ventilation injury–induced and bleomycin-induced lung injury (36–38). Like our results, these observations suggest that PAR1 signaling contributes to inflammatory responses to injury in the lung, the major target in our IAV infection model.

PAR1 activation did not exacerbate the effects of IAV infection in *Plg*$^{-/-}$ mice (Figure 3). It is possible that PLG is simply playing a permissive role for the effect of PAR1 activation in IAV infection; that is, PLG supports infection and injury, and PAR1 activation exacerbates their effects. Interestingly, however, PAR1-AP did promote PLG-dependent HA cleavage in lung epithelial cultures, suggestive of a possible interaction of PAR1 signaling with the ability of IAV to become infectious and hence replicate. These findings are consistent with the prior observation that PLG contributes to the pathogenesis of IAV infection (27, 28). Additionally, PAR1 signaling may promote PLG activation to plasmin (29, 30), thereby providing a possible link to increased HA cleavage and IAV production. It is also possible that PAR1 activation contributes to proinflammatory functions of PLG (25, 39–41), by promoting its conversion to plasmin or by other mechanisms.

Additional considerations suggest that PAR1 activation's abilities to promote early virus replication and to enhance a harmful inflammatory response in the respiratory tract are, at least in part, independent of each other. When PAR1-AP was delivered 3 days after infection, despite similar virus replication in the lungs, treatment still had a deleterious effect (data not shown). Additionally, based on critical residues in HA involved for cleavage by plasmin, it is unlikely that the replication of highly pathogenic H5N1 and 2009 pandemic H1N1 are modulated by plasmin (42), yet SCH79797 treatment still decreased mortality.

As noted above, we found that in IAV-infected A549 cells, activation of PAR1 increased PLG-dependent HA cleavage, an essential step for virus infectivity. Indeed, only the cleaved form of HA permits pH-dependent fusion of the viral envelope within the endosomal membranes and subsequent release of the genome into the cytosol and virus replication. In vivo, PAR1 also promoted virus replication shortly after infection. However, at 48 hours after infection, no difference in lung virus titers was observed between PAR1-AP–stimulated and unstimulated mice, which suggests that HA cleavage could be compensated by other proteases that are either recruited or activated by infection in the lungs.

Therefore, we propose a model (Figure 7) in which PAR1 promotes activation of PLG into plasmin. Subsequently, plasmin acts on virus replication through HA cleavage, enhancement of which likely enhances inflammation via pathogen-associated molecular patterns. Simultaneously, plasmin also acts as a proinflammatory mediator that accounts for the deleterious lung inflammation. Additionally, PAR1 triggers a variety of proinflammatory responses,

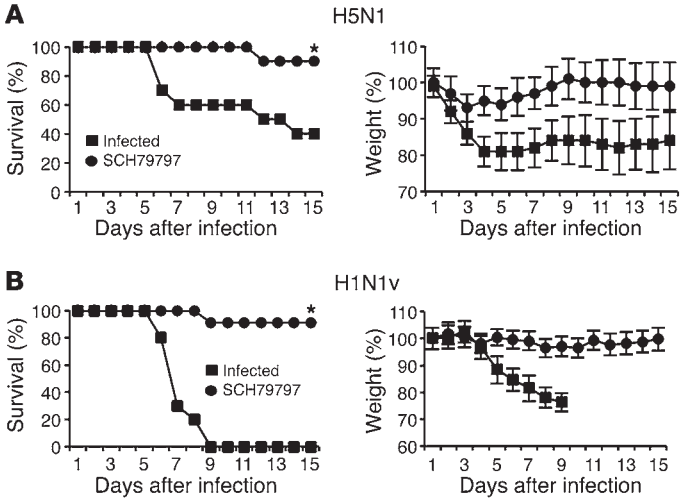

Figure 6
PAR1 antagonist protects mice from lethal infection with H5N1 or H1N1v. Mice were inoculated intranasally with (**A**) 5,000 PFU H5N1 (n = 10 per group) or (**B**) 500 PFU H1N1v (n = 10–11 per group) and treated or not with 50 μM SCH79797. Results are expressed as percent survival or weight loss from 2 experiments. *P < 0.05, treated vs. control, Kaplan-Meier test.

independent of PLG and virus, that may exacerbate inflammation and injury. Because PAR1 couples coagulation to inflammation (14, 15) and coagulation to fibrinolysis (30), further studies are needed to investigate the overall impact of hemostasis dysregulation in PAR1-mediated inflammation during IAV infection.

Our observation that a PAR1 agonist (43, 44) exacerbated the effects of IAV infection suggests that PAR1 activation is capable of promoting inflammation and tissue damage in this setting. Moreover, our observation that *Par1*$^{-/-}$ mice and SCH79797-treated mice were protected from IAV infection suggests that PAR1 activation contributes to the pathogenesis of IAV infection and that PAR1 is endogenously activated during IAV infection. Accordingly, the natural PAR1 activator thrombin was generated in IAV-infected lungs (45), and elevated levels of PAR1 were observed in the airways of IAV-infected mice (17). It is worth noting, however, that SCH79797 is known to have off-target effects on cell proliferation and survival (46, 47); thus, we cannot exclude PAR1-independent effect of SCH79797. However, SCH79797 was capable of inhibiting PAR1 signaling (Figure 4A and ref. 18), and the concordance of our KO and inhibitor studies — and the fact that their effects were opposite from those of PAR1-AP — suggest that the effects of SCH79797 in our model could be related to its ability to block PAR1 signaling.

Besides PAR1, other PARs may be involved in the pathogenesis of IAV infection (48–50). Identification of the exact nature and amount of proteases present at the site of infection, and how virus strain differences alter the immune response and its interactions with PARs, may advance our understanding of the pathogenesis of IAV infection.

Current treatments for IAV infection target the viral proteins M2 and NA. These drugs suffer from a number of disadvantages, including the rapid development of resistant virus variants as a result of selective pressure, which highlights the need for new pharmacological strategies against IAV infection. Because targeting host proteins would not be subject to resistance, and because severe infections with IAV are associated with a deleterious host inflammatory response, drugs regulating inflammation are appealing as potential treatments for IAV infection (51, 52). In our present study, blocking PAR1 signaling almost fully protected mice from a highly pathogenic, oseltamivir-resistant 2009 pandemic H1N1v virus isolated from a severely diseased oseltamivir-treated patient (34). Additionally, inhibition of PAR1 signaling up to 3 days after inoculation protected mice from a detrimental outcome of infection with various IAVs, including H1N1 and H3N2 strains. Because IAVs of the H1N1 and H3N2 subtypes are currently circulating in the human population, it is reasonable to assume that PAR1 antagonists are most likely also effective against seasonal influenza viruses. Interestingly, the PAR1 antagonist vorapaxar has been studied as a potential antithrombotic drug in approximately 40,000 patients over 3 years (53, 54). The most serious side effect, increased incidence of intracranial bleeding, occurred mainly in patients with a history of prior stroke. In the absence of such a history, the increase in the incidence of intracranial bleeding was less than 1 per 1,000 treatment-years. Thus, short periods of PAR1 antagonism would appear to be relatively safe. This observation, in consideration with our results, suggests that PAR1 antagonism

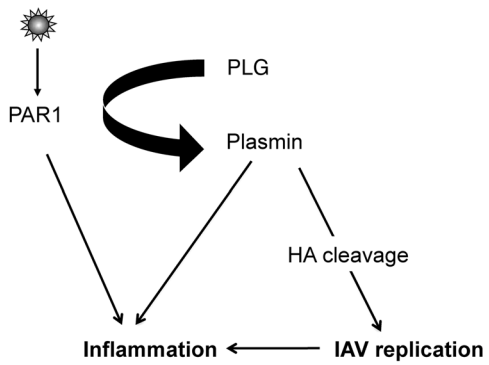

Figure 7
Proposed model for PAR1-mediated influenza virus pathogenesis. During IAV infection, PAR1 is activated and increases conversion of PLG into plasmin. On the one hand, plasmin cleaves and activates the viral HA, promoting IAV replication, which contributes to inflammation. On the other hand, plasmin directly promotes inflammation, and PAR1 promotes inflammation via mechanisms that are independent of PLG and virus. These likely interact with other host responses to viral infection to exacerbate inflammation and injury.

should be further explored for the treatment of IAV in additional preclinical models and, if appropriate, human studies.

Methods

Cells, virus strain, and reagents. The NIH3T3 mouse cell line was a gift from D. Décimo (INSERM U758, Lyon, France). The human alveolar type II (A549) and MDCK cell lines used in this study were obtained from ATCC and grown as previously described (55). H1N1 (strain A/PR/8/34) was obtained from the ATCC. H3N2 (strain A/Hong-Kong/2/68) was obtained from the Dutch National Influenza Centre. The strain was originally obtained from the National Institute for Biological Standards and Control (NIBSC). The highly pathogenic H5N1 avian influenza virus (strain A/mallard/Bavaria/1/2006; also known as MB1) and the pandemic H1N1v influenza virus (strain A/Nordrhein-Westfalen/173/09) were used in this study. H1N1v, isolated from a severe H1N1pdm09 case and obtained through the German National Reference Centre for Influenza of the Robert Koch Institute, had acquired oseltamivir resistance during treatment (34). H5N1 was propagated in chicken eggs for 2 days, and the other viruses were propagated in confluent MDCK cells. After 2 days, cytopathic changes were complete, and culture supernatants were harvested and cleared by low-speed centrifugation and stored at –80°C. PAR1-AP and control peptide (TFLLR-NH_2 and FTLLR-NH_2, respectively) were purchased from Bachem. The PAR1 antagonist (SCH79797 dihydrochloride) was purchased from Axon Medchem. PLG was purchased from Sigma-Aldrich, and the following antibodies were used: monoclonal anti-HA (C102; Santa Cruz Biotechnology), monoclonal anti-tubulin (Sigma-Aldrich), and polyclonal anti-ERK and phospho-ERK (Cell Signaling Technology).

In vitro stimulation. A549 cells were preincubated for 5 minutes with 40 μM PAR1-AP or control peptide or for 1 hour with 5 μM SCH79797. Cells were then infected with H1N1 (MOI 0.001) in MEM supplemented with 0.5 μM PLG (Sigma-Aldrich) in the presence of the drug. At the indicated times after stimulation, virus titers were analyzed by classical plaque assays as performed previously, using MDCK cells (56).

Western blot analysis of ERK activation and HA cleavage. A549 or NIH3T3 cells were stimulated or not with the indicated concentrations of PAR1-AP for 5 minutes at 37°C. Where indicated, cells were preincubated for 1 hour with SCH79797. Cells were then lysed, and proteins from the lysate were analyzed by Western blot for ERK activation, as previously described (57). For the HA cleavage experiments, A549 cells were stimulated or not with 40 μM PAR1-AP and infected with IAV (MOI 0.5) for 16 hours in the presence or absence of 0.5 μM PLG. Cells were then lysed, and proteins from the lysate were analyzed by Western blot, as described previously (57).

Mice. $Plg^{-/-}$ mice (with a disrupted *Plg* gene) and their WT littermates (58) and 6-week-old C57BL/6 female mice (Charles River Laboratories) were used in this study. $Par1^{-/-}$ mice (with a disrupted *Par1* gene) and their WT littermates were described previously (59). Heterozygous mice were crossed, and WT and KO offspring were used. Mouse ages ranged from 5 weeks to a maximum of 4 months, since the number of mice that could be obtained was limited. Male and female mice were used in the experiments. Groups of WT and KO mice were stratified for these differences in age and gender. Polymerase chain reaction of tail-tip genomic DNA was performed (60) for determination of the absence or presence of a functional *Plg* or *Par1* gene.

Mouse infection and treatment. Mice were anesthetized and inoculated intranasally with 25 μl of a solution containing different doses of virus in the presence or absence of 50 μM PAR1-AP, 50 μM control peptide, and/or 50 μM SCH79797. 500 μM SCH79797 was also used for blocking experiments in Figure 4B. Intranasal treatments with PAR1-AP, control peptide, and/or SCH79797 were also repeated at days 2 and 3 after infection. Alternatively, mice were inoculated, and SCH79797 was administered on days 2–4 or days 3–5 after infection. Mice were then monitored for weight loss and mortality. For assessing virus replication, lungs were obtained from scarified mice, and infectious virus titers were determined by plaque assay as described previously (56).

Cytokine detection by ELISA and PMN recruitment. Production of the cytokines RANTES, IL-6, and KC in the lungs was determined by ELISA (R&D Systems), using BAL from mice, as previously described (60). For PMN recruitment, BAL was collected in PBS (Invitrogen) supplemented with 1 mM EDTA (Invitrogen). After cytocentrifugation, the percentage of PMNs was determined by counting a total of 500 cells per sample by microscopic examination of May-Grünwald– and Giemsa-stained cytocentrifuge slides.

Lung histology. At 3 days after virus inoculation and treatment, mice were killed, and lung tissue was harvested, fixed in 10% formaldehyde, and subsequently embedded in paraffin. Tissues were sectioned at 12 μM, and sections were examined after staining with hematoxylin and eosin for histopathological changes.

Statistics. Mann-Whitney test was used for statistical analysis of lung virus titers and cytokine ELISA results. Kaplan-Meier test was used for statistical analysis of survival rates. XLSTAT software was used to analyze differences between groups; a P value less than 0.05 was considered statistically significant.

Study approval. Experiments were performed according to recommendations of the National Commission of Animal Experiment (CNEA) and the National Committee on the Ethic Reflexion of Animal Experiments (CNREEA) in compliance with European animal welfare regulation. The protocol was approved by the committee of animal experiments of the University Claude Bernard Lyon I (permit no. BH2008-13). All animal experiments were also carried out under the authority of licence issued by "la direction des services Vétérinaires" (accreditation no. 78-114). All efforts were made to minimize suffering.

Acknowledgments

We are grateful to N. Lejal for technical assistance. This work was supported by the Agence Nationale de la Recherche (ANR; to B. Riteau); Inserm Avenir (to E. Camerer); Marie Curie actions (to E. Camerer); and Long-term structural funding—Methusalem by the Flemish government (to P. Carmeliet).

Received for publication November 7, 2011, and accepted in revised form October 4, 2012.

Address correspondence to: Beatrice Riteau, EMR 4610 Vir-Path, Virologie et Pathologie Humaine, Faculté de médecine RTH Laennec, Université Claude Bernard Lyon 1, Université de Lyon, F-69008, Lyon, France. Phone: 33.1.0478771008; Fax: 33.1.0478778751; E-mail: beatrice.riteau@univ-lyon1.fr.

1. La Gruta NL, Kedzierska K, Stambas J, Doherty PC. A question of self-preservation: immunopathology in influenza virus infection. *Immunol Cell Biol*. 2007;85(2):85–92.
2. Bouvier NM, Palese P. The biology of influenza viruses. *Vaccine*. 2008;26(suppl 4):D49–D53.
3. Kuiken T, Riteau B, Fouchier RA, Rimmelzwaan GF. Pathogenesis of influenza virus infections: the good, the bad and the ugly. *Curr Opin Virol*. 2012;2(3):276–286.
4. Webby RJ, Webster RG. Are we ready for pandemic influenza? *Science*. 2003;302(5650):1519–1522.
5. Foucault ML, Moules V, Rosa-Calatrava M, Riteau B. Role for proteases and HLA-G in the pathogenicity of influenza A viruses. *J Clin Virol*. 2011;51(3):155–159.
6. Solorzano A, Song H, Hickman D, Perez DR. Pandemic influenza: preventing the emergence of novel strains and countermeasures to ameliorate its effects. *Infect Disord Drug Targets*. 2007;7(4):304–317.
7. Schmolke M, Garcia-Sastre A. Evasion of innate and adaptive immune responses by influenza A virus. *Cell Microbiol*. 2010;12(7):873–880.
8. de Jong MD, et al. Fatal outcome of human influenza A (H5N1) is associated with high viral load and hypercytokinemia. *Nat Med*. 2006;12(10):1203–1207.
9. Peiris JS, Cheung CY, Leung CY, Nicholls JM. Innate

immune responses to influenza A H5N1: friend or foe? *Trends Immunol*. 2009;30(12):574–584.
10. Heutinck KM, ten Berge IJ, Hack CE, Hamann J, Rowshani AT. Serine proteases of the human immune system in health and disease. *Mol Immunol*. 2010;47(11–12):1943–1955.
11. Mackie EJ, Pagel CN, Smith R, de Niese MR, Song SJ, Pike RN. Protease-activated receptors: a means of converting extracellular proteolysis into intracellular signals. *IUBMB Life*. 2002;53(6):277–281.
12. Hollenberg MD. Proteinase-mediated signaling: proteinase-activated receptors (PARs) and much more. *Life Sci*. 2003;74(2–3):237–246.
13. Riteau B, de Vaureix C, Lefevre F. Trypsin increases pseudorabies virus production through activation of the ERK signalling pathway. *J Gen Virol*. 2006;87(pt 5):1109–1112.
14. Vu TK, Hung DT, Wheaton VI, Coughlin SR. Molecular cloning of a functional thrombin receptor reveals a novel proteolytic mechanism of receptor activation. *Cell*. 1991;64(6):1057–1068.
15. Coughlin SR. Thrombin signalling and protease-activated receptors. *Nature*. 2000;407(6801):258–264.
16. Coughlin SR, Camerer E. PARticipation in inflammation. *J Clin Invest*. 2003;111(1):25–27.
17. Lan RS, Stewart GA, Goldie RG, Henry PJ. Altered expression and in vivo lung function of protease-activated receptors during influenza A virus infection in mice. *Am J Physiol Lung Cell Mol Physiol*. 2004;286(2):L388–L398.
18. Ahn HS, Foster C, Boykow G, Stamford A, Manna M, Graziano M. Inhibition of cellular action of thrombin by N3-cyclopropyl-7-[[4-(1-methylethyl) phenyl]methyl]-7H-pyrrolo[3, 2-f]quinazoline-1,3-diamine (SCH 79797), a nonpeptide thrombin receptor antagonist. *Biochem Pharmacol*. 2000; 60(10):1425–1434.
19. Goto S, Yamaguchi T, Ikeda Y, Kato K, Yamaguchi H, Jensen P. Safety and exploratory efficacy of the novel thrombin receptor (PAR-1) antagonist SCH530348 for non-ST-segment elevation acute coronary syndrome. *J Atheroscler Thromb*. 2010;17(2):156–164.
20. White HD. Oral antiplatelet therapy for atherothrombotic disease: current evidence and new directions. *Am Heart J*. 2011;161(3):450–461.
21. Oestreich J. SCH-530348, a thrombin receptor (PAR-1) antagonist for the prevention and treatment of atherothrombosis. *Curr Opin Investig Drugs*. 2009;10(9):988–996.
22. Shinohara Y, Goto S, Doi M, Jensen P. Safety of the novel protease-activated receptor-1 antagonist vorapaxar in Japanese patients with a history of ischemic stroke. *J Stroke Cerebrovasc Dis*. 2012;21(4):318–324.
23. LeBouder F, Lina B, Rimmelzwaan GF, Riteau B. Plasminogen promotes Influenza A virus replication through an annexin II-dependent pathway in absence of neuraminidase. *J Gen Virol*. 2010; 91(pt 11):2753–2761.
24. LeBouder F, et al. Annexin II incorporated into influenza virus particles supports virus replication by converting plasminogen into plasmin. *J Virol*. 2008;82(14):6820–6828.
25. Wygrecka M, et al. Enolase-1 promotes plasminogen-mediated recruitment of monocytes to the acutely inflamed lung. *Blood*. 2009;113(22):5588–5598.
26. Gong Y, Hart E, Shchurin A, Hoover-Plow J. Inflammatory macrophage migration requires MMP-9 activation by plasminogen in mice. *J Clin Invest*. 2008;118(9):3012–3024.
27. Goto H, Wells K, Takada A, Kawaoka Y. Plasminogen-binding activity of neuraminidase determines the pathogenicity of influenza A virus. *J Virol*. 2001; 75(19):9297–9301.
28. Goto H, Kawaoka Y. A novel mechanism for the acquisition of virulence by a human influenza A virus. *Proc Natl Acad Sci U S A*. 1998;95(17):10224–10228.
29. Peterson EA, Sutherland MR, Nesheim ME, Pryzdial EL. Thrombin induces endothelial cell-surface exposure of the plasminogen receptor annexin 2. *J Cell Sci*. 2003;116(pt 12):2399–2408.
30. McEachron TA, Pawlinski R, Richards KL, Church FC, Mackman N. Protease-activated receptors mediate crosstalk between coagulation and fibrinolysis. *Blood*. 2010;116(23):5037–5044.
31. Strande JL, Hsu A, Su J, Fu X, Gross GJ, Baker JE. SCH 79797, a selective PAR1 antagonist, limits myocardial ischemia/reperfusion injury in rat hearts. *Basic Res Cardiol*. 2007;102(4):350–358.
32. Cao C, Gao Y, Li Y, Antalis TM, Castellino FJ, Zhang L. The efficacy of activated protein C in murine endotoxemia is dependent on integrin CD11b. *J Clin Invest*. 2010;120(6):1971–1980.
33. Lo HM, Chen CL, Tsai YJ, Wu PH, Wu WB. Thrombin induces cyclooxygenase-2 expression and prostaglandin E2 release via PAR1 activation and ERK1/2- and p38 MAPK-dependent pathway in murine macrophages. *J Cell Biochem*. 2009; 108(5):1143–1152.
34. Seyer R, et al. Synergistic adaptive mutations in the HA and PA lead to increased virulence of pandemic 2009 H1N1 influenza A virus in mice. *J Infect Dis*. 2012;205(2):262–271.
35. Su X, Camerer E, Hamilton JR, Coughlin SR, Matthay MA. Protease-activated receptor-2 activation induces acute lung inflammation by neuropeptide-dependent mechanisms. *J Immunol*. 2005; 175(4):2598–2605.
36. Jenkins RG, et al. Ligation of protease-activated receptor 1 enhances alpha(v)beta6 integrin-dependent TGF-beta activation and promotes acute lung injury. *J Clin Invest*. 2006;116(6):1606–1614.
37. Mercer PF, Deng X, Chambers RC. Signaling pathways involved in proteinase-activated receptor1-induced proinflammatory and profibrotic mediator release following lung injury. *Ann N Y Acad Sci*. 2007;1096:86–88.
38. Chen D, et al. Protease-activated receptor 1 activation is necessary for monocyte chemoattractant protein 1-dependent leukocyte recruitment in vivo. *J Exp Med*. 2008;205(8):1739–1746.
39. Busuttil SJ, Ploplis VA, Castellino FJ, Tang L, Eaton JW, Plow EF. A central role for plasminogen in the inflammatory response to biomaterials. *J Thromb Haemost*. 2004;2(10):1798–1805.
40. Syrovets T, Tippler B, Rieks M, Simmet T. Plasmin is a potent and specific chemoattractant for human peripheral monocytes acting via a cyclic guanosine monophosphate-dependent pathway. *Blood*. 1997;89(12):4574–4583.
41. O'Connell PA, Surette AP, Liwski RS, Svenningsson P, Waisman DM. S100A10 regulates plasminogen-dependent macrophage invasion. *Blood*. 2010; 116(7):1136–1146.
42. Sun X, Tse LV, Ferguson AD, Whittaker GR. Modifications to the hemagglutinin cleavage site control the virulence of a neurotropic H1N1 influenza virus. *J Virol*. 2010;84(17):8683–8690.
43. Zhao A, et al. Immune regulation of protease-activated receptor-1 expression in murine small intestine during Nippostrongylus brasiliensis infection. *J Immunol*. 2005;175(4):2563–2569.
44. Cunningham MA, Rondeau E, Chen X, Coughlin SR, Holdsworth SR, Tipping PG. Protease-activated receptor 1 mediates thrombin-dependent, cell-mediated renal inflammation in crescentic glomerulonephritis. *J Exp Med*. 2000;191(3):455–462.
45. Keller TT, et al. Effects on coagulation and fibrinolysis induced by influenza in mice with a reduced capacity to generate activated protein C and a deficiency in plasminogen activator inhibitor type 1. *Circ Res*. 2006;99(11):1261–1269.
46. Di Serio C, et al. Protease-activated receptor 1-selective antagonist SCH79797 inhibits cell proliferation and induces apoptosis by a protease-activated receptor 1-independent mechanism. *Basic Clin Pharmacol Toxicol*. 2007;101(1):63–69.
47. Pawlinski R, et al. Response to letter by Strande regarding article "Protease-activated receptor-1 contributes to cardiac remodeling and hypertrophy". *Circulation*. 2008;117(24):e496.
48. Khoufache K, et al. Protective role for protease-activated receptor-2 against influenza virus pathogenesis via an IFN-gamma-dependent pathway. *J Immunol*. 2009;182(12):7795–7802.
49. Nhu QM, et al. Novel signaling interactions between proteinase-activated receptor 2 and Toll-like receptors in vitro and in vivo. *Mucosal Immunol*. 2010; 3(1):29–39.
50. Feld M, et al. Agonists of proteinase-activated receptor-2 enhance IFN-gamma-inducible effects on human monocytes: role in influenza A infection. *J Immunol*. 2008;180(10):6903–6910.
51. Garcia CC, et al. Platelet-activating factor receptor plays a role in lung injury and death caused by Influenza A in mice. *PLoS Pathog*. 2010;6(11):e1001171.
52. Walsh KB, et al. Suppression of cytokine storm with a sphingosine analog provides protection against pathogenic influenza virus. *Proc Natl Acad Sci U S A*. 2011;108(29):12018–12023.
53. Tricoci P, et al. Thrombin-receptor antagonist vorapaxar in acute coronary syndromes. *N Engl J Med*. 2012;366(1):20–33.
54. Morrow DA, et al. Vorapaxar in the secondary prevention of atherothrombotic events. *N Engl J Med*. 2012;366(15):1404–1413.
55. Riteau B, et al. Characterization of HLA-G1, -G2, -G3, and -G4 isoforms transfected in a human melanoma cell line. *Transplant Proc*. 2001;33(3):2360–2364.
56. LeBouder F, et al. Immunosuppressive HLA-G molecule is upregulated in alveolar epithelial cells after influenza A virus infection. *Hum Immunol*. 2009;70(12):1016–1019.
57. Riteau B, Barber DF, Long EO. Vav1 phosphorylation is induced by beta2 integrin engagement on natural killer cells upstream of actin cytoskeleton and lipid raft reorganization. *J Exp Med*. 2003; 198(3):469–474.
58. Ploplis VA, et al. Effects of disruption of the plasminogen gene on thrombosis, growth, and health in mice. *Circulation*. 1995;92(9):2585–2593.
59. Griffin CT, Srinivasan Y, Zheng YW, Huang W, Coughlin SR. A role for thrombin receptor signaling in endothelial cells during embryonic development. *Science*. 2001;293(5535):1666–1670.
60. Bernard D, et al. Costimulatory receptors in a teleost fish: typical CD28, elusive CTLA4. *J Immunol*. 2006;176(7):4191–4200.